The Conformational Properties of Elongation Factor G and the Mechanism of Translocation†

John Czworkowski and Peter B. Moore*

Departments of Chemistry, and Molecular Biophysics and Biochemistry, Yale University, P.O. Box 208107, New Haven, Connecticut 06520-8107

Received March 17, 1997; Revised Manuscript Received June 6, 1997⊗

ABSTRACT: The elongation phase of protein synthesis is promoted by two G proteins, elongation factor Tu (EF-Tu), which delivers aminoacyl tRNAs to the ribosome, and elongation factor G (EF-G), which catalyzes translocation. Crystallographic investigations have revealed that EF-G·GDP resembles the EF-Tu·GTP·(aminoacyl tRNA) complex, and it has been proposed that the translocase function of EF-G is derived from this similarity [Nissen, P., et al. (1995) *Science* 270, 1464]. However, its significance is uncertain because the affinity of EF-G·GDP for the ribosome is much lower than that of the ternary complex it resembles and because EF-Tu·GDP, the form of EF-Tu that has low ribosome affinity, has a conformation radically different from that of EF-Tu·GTP or EF-Tu in the ternary complex. The small-angle X-ray scattering study described here was undertaken to ascertain if the form of EF-G that has high ribosome affinity, EF-G·GTP, the structure of which is unknown, could be a mimic of EF-Tu·GDP. The data show that nucleotide-free EF-G, EF-G·GDP, EF-G·GTP, and EF-G·GMPPCP cannot be distinguished by solution scattering and that it is likely they all resemble crystalline EF-G·GDP. Since an EF-Tu-like change would easily have been detected, it follows that it does not occur in EF-G. These observations have significant implications for the mechanism of translocation.

The elongation cycle phase of protein synthesis is promoted by two proteins that perform complementary functions. The first, which is called elongation factor Tu (EF-Tu)[1] in bacteria, loads aminoacyl tRNAs into the A site of ribosomes that have mRNAs bound, empty A sites, and peptidyl tRNAs in their P sites. Immediately following the departure of EF-Tu from a ribosome, the peptide bound to the tRNA in its P site is transferred to the amino acid bound to its A-site tRNA, and at that point, the second protein, elongation factor G (EF-G), comes into play. It helps evict the newly deacylated tRNA from the P site, advances the ribosome down its mRNA by one codon, and clears the A site by moving the peptidyl tRNA it contains to the P site. The EF-G-promoted step is called translocation.

EF-Tu and EF-G are similar in many respects. They bind to the same site on the ribosome (Bodley & Lin, 1970; Richter, 1972; Miller, 1972; Richman & Bodley, 1972), and both possess a GTPase activity that is dramatically activated by ribosome binding. They bind to the ribosome with high affinity when associated with GTP, and their affinities drop dramatically when GDP is bound. Sequence comparisons done many years ago revealed that their first domains are homologous to each other and to the GTP-binding domains of other G proteins (Bourne et al., 1991). Three years ago, when the crystal structures of apo-EF-G and EF-G·GDP were determined, it became apparent that the second domains of EF-Tu and EF-G are homologous also (Ævarsson et al., 1994; Czworkowski et al., 1994). A year later, it was discovered that the third, fourth, and fifth domains of EF-G·GDP, which have no homologues in EF-Tu, together resemble a tRNA, and that EF-G looks like EF-Tu·GTP·(aminoacyl tRNA) (the ternary complex) (Nissen et al., 1995). This observation led to the hypothesis that EF-G functions as a molecular mimic of the ternary complex.

Some aspects of the mimicry hypothesis are puzzling. For example, the ternary complex binds to ribosomes with high affinity, but EF-G·GDP, the protein it resembles, does not. Given this critical functional difference, what does their similarity mean? Further, EF-Tu·GTP undergoes a huge conformational change when its GTP is hydrolyzed to GDP; its second and third domains move away from and change orientation with respect to its G domain (Kjeldgaard & Nyborg, 1992; Kjeldgaard et al., 1993; Berchtold et al., 1993). If EF-G·GDP resembles the ternary complex, could it be that EF-G·GTP resembles EF-Tu·GDP? Since functions performed by the two molecules are complementary, it does not seem far-fetched to postulate that they undergo complementary conformational changes (Liljas, 1996).

Below we report the results of a small-angle X-ray scattering (SAXS) study that compares the conformations of nucleotide-free (apo-)EF-G, EF-G·GDP, EF-G·GTP, and EF-G·GMPPCP in solution. The radii of gyration and the length distributions of these four forms of EF-G are the same within experimental uncertainty and indistinguishable from that predicted assuming their conformations in solution are the same as crystalline EF-G·GDP. Since modeling studies show that a conformational change in EF-G similar to that documented for EF-Tu would easily have been detected, we

† This work was supported by grants from the National Institutes of Health (AI09167 and GM54216 to P.B.M.; GM22778 to T.A.S.).

* Author to whom correspondence should be addressed.

⊗ Abstract published in *Advance ACS Abstracts,* August 1, 1997.

[1] Abbreviations: DTT, dithiothreitol; EDTA, ethylenediaminetetraacetic acid; EF-G, elongation factor G; EF-Tu, elongation factor Tu; GMPPCP, guanosine 5′-[β,γ-methylene]triphosphate; HEPES, 4-(2-hydroxyethyl)piperazine-1-ethanesulfonic acid; HPLC, high-pressure liquid chromatography; IPTG, isopropyl β-D-thiogalactoside; PDB, Protein Data Bank; PMSF, phenylmethylsulfonyl fluoride; SAXS, small-angle X-ray scattering; Tris, tris(hydroxymethyl)aminomethane.

S0006-2960(97)00610-7 CCC: $14.00

conclude that the gross conformation of EF-G is insensitive to the identity of the guanine nucleotide bound to it. Thus to the extent that EF-G·GDP is a mimic of the EF-Tu ternary complex, EF-G·GTP, the high-affinity form of EF-G, must be a mimic also. Taken together with the many other facts available, this observation suggests a mechanism for translocation, which is discussed below.

EXPERIMENTAL PROCEDURES

Purification of EF-G. EF-G from *Thermus thermophilus* was overexpressed in *Escherichia coli* strain JM109 from pfus1, a plasmid given to us by Dr. Matthias Sprinzl (Blank et al., 1995). Transformed cells were resurrected from a glycerol freeze in a small volume of M9 medium (Maniatis et al., 1982) supplemented with 4 mg/mL glucose, 0.32 mg/mL $MgSO_4$, 0.1 mg/mL thiamine, and 0.1 mg/mL ampicillin. Cells were then grown at 37 °C in LB medium (Maniatis et al., 1982) containing 75 μg/mL ampicillin to an OD_{550nm} of 0.6, at which point they were induced by addition of IPTG to a concentration of 1.0 mM. All subsequent steps in the purification were carried out at 4 °C.

A 10 g amount of wet cells was ground with 25 g of alumina, and the lysate was resuspended in 40 mL of buffer solution A (50 mM Tris-HCl, 5 mM EDTA, 5% v/v glycerol, 1 mM 2-mercaptoethanol and 100 μM PMSF, pH 7.5). A 5 mg amount of lysozyme was added, and the suspension was kept on ice for an additional 30 min. The concentration of $MgCl_2$ was then adjusted to 20 mM, ca. 5 mg of DNase I was added, and the mixture was stirred on ice for 30 min. Alumina and cell debris were removed by centrifugation at 9600*g* for 20 min. The alumina pellet was washed with an additional 40 mL of buffer solution A, the suspension was recentrifuged and the supernatants were pooled. Ribosomes were removed by centrifugation at 255000*g* for 1.5 h. The supernatant was then heated to 65 °C for 20 min. The sample was cooled and centrifuged at 11300*g* for 25 min to remove denatured *E. coli* proteins. Ammonium sulfate (44 g) was added per every 100 mL of solution, and the protein was allowed to precipitate overnight. The ammonium sulfate precipitate was recovered by centrifugation and resuspended in a small volume of buffer B (50 mM Tris-HCl, 10 mM $MgCl_2$, 2 mM 2-mercaptoethanol, and 100 μM PMSF, pH 7.5). The solution was fractionated on a Sephacryl S-200 column equilibrated with the same buffer. The fractions containing EF-G, which were identified by SDS gel electrophoresis, were pooled and recovered by ammonium sulfate precipitation. The pellet was dissolved in a small amount of buffer C (50 mM Tris-HCl, 10 mM $MgCl_2$, 1 mM NaN_3, 0.5 mM DTT, and 10 μM PMSF, pH 7.6) and dialyzed against the same buffer. The final step was fractionation on a DEAE-Sepharose Cl-6B column equilibrated with buffer C, with a NaCl gradient from 0.0 to 0.3 M. Fractions containing EF-G, which were pure as judged by using silver-stained SDS gels, were pooled, concentrated by ultrafiltration, and dialyzed against scattering buffer (100 mM KCl, 5 mM $MgCl_2$, 1 mM DTT, 1 mM NaN_3, 20 mM HEPES-KOH, pH 7.4). The total yield was 2.8 mg of EF-G per gram of cells.

The molar absorptivity of the protein at 280 nm, ϵ_{280}^{M}, was determined to be 49800 M^{-1} cm^{-1} by the method of Gill and von Hippel (1989); the corresponding value of $\epsilon_{280}^{0.1\%}$ is 0.647 L g^{-1} cm^{-1}.

Guanine Nucleotide Purity. Nucleotide preparations were analyzed by HPLC on Vydac 301VHP and 303NT columns. For the Vydac 301VHP column, solvent A was water and solvent B was 1.0 M ammonium acetate, pH 7.5. The gradient used was 0−12% B. The Vydac 303NT column was run as recommended by the manufacturer: solvent A was 0.045 M ammonium formate, pH 4.5, and solvent B was 0.5 M sodium phosphate, the pH of which was set to 2.7 with formic acid; the gradient run was 0−100% B.

Nucleotide Content of EF-G Preparations. Aliquots of protein were extracted three times with 1:1 phenol:chloroform that had been equilibrated against a solution of 20 mM HEPES-KOH, 100 mM KCl, pH 7.4. Pooled aqueous layers were then extracted four times with chloroform and analyzed on a Vydac 303NT column as described above. The EF-G used for these experiments contained no detectable guanine nucleotide. Control experiments demonstrated that a 2% (mole/mole) nucleotide contamination in the protein sample would have been detected.

Nucleotide Binding. Nucleotide binding was measured by observing the retention of EF-G·[^{3}H]GDP complexes on nitrocellulose filters (Millipore HAWP). The binding of [^{3}H]-GDP (Dupont NEN) to EF-G was determined by measuring radioactivity retained after passing solutions of constant EF-G concentration and varying GDP concentration through filters. The buffer was that used for X-ray scattering (100 mM KCl, 20 mM HEPES-KOH, 5 mM $MgCl_2$, 1 mM DTT, and 1 mM NaN_3). Nucleotide−protein mixtures were incubated for 30 min at 30 °C and chilled immediately before filtration. After samples were passed through the filters, the filters were rinsed with a small volume of ice-cold buffer solution. The binding of GTP and GMPPCP to EF-G was evaluated by measuring the capacity of nonradioactive nucleotides to compete with [^{3}H]GDP for EF-G. EF-G, which was nearly saturated with GDP, was challenged with increasing concentrations of unlabeled GTP and GMPPCP. The best values for the dissociation constants were found by nonlinear least-squares fit to the appropriate equations [see Winzor and Sawyer (1995) and Rose and Hogg (1995)] using the program Mathematica (Wolfram Research, Inc.).

SAXS Samples. A stock solution of nucleotide-free *T. thermophilus* EF-G was prepared at a concentration of 12.8 g/L in SAXS buffer. Samples containing no nucleotide, GDP at 1 mM, or GMPPCP at 3 mM were prepared from this stock solution with EF-G in the concentration range 2.1−11.4 g/L. Samples containing the GTP regeneration system contained 1 mM guanine nucleotide and EF-G at 2−6 g/L. All samples were in SAXS buffer, and their scattering was measured was measured at 21 °C.

GDP, which was both an initial contaminant and a hydrolysis product, was converted back to GTP in the SAXS samples in which EF-G·GTP was to be studied using a regeneration system like those of Arai et al. (1974) and Österberg et al. (1981). In addition to EF-G, GTP, and SAXS buffer, the samples contained 8 nM rabbit-muscle pyruvate kinase (Sigma, salt-free lyophilized) and 5 mM 2-phospho(enol)pyruvate (PEP) (Calbiochem, trisodium salt). Under these conditions a 1-mM solution of GDP is completely converted to GTP in 1 h.

X-ray Data Collection and Processing. The small-angle scattering instrument used had pin-hole collimation with an incident beam diameter of 1.2 mm and was equipped with a Rigaku RU-300 rotating anode generator and a Hamlin

multiwire detector [see Smith et al. (1996)]. Data collection times were typically 5−9 h per sample. Scattering profiles were determined by circular averaging of the two-dimensional data obtained about the optical axis of the instrument. Small angle spectrometers with pin-hole optics collect data that are almost unaffected by slit-smearing aberrations. Since computational trials confirmed that slit-smearing effects were negligible, none of the data reported here was corrected for it.

Scattering profiles were Fourier-inverted to give length distributions by using a method described previously (Moore, 1980). The $\ln(I(q))$ was plotted against $\ln(q)$ so that the Porod's Law region, where $I(q)$ is proportional to q^{-4}, could be identified (Porod, 1951). Data sets were truncated at the high-angle end of this region, and truncation effects were corrected for by assuming that Porod's Law holds to $q = \infty$ [see Moore (1980)]. The maximum distance allowed in computed length distributions was determined by examining the dependence on maximum distance of the χ^2 value of the fit of predicted scattering curves to the measured data. The shortest distance that gave a good fit was chosen. Both the instrument and the approach taken to data processing were tested on data obtained from solutions of bovine serum albumin. The radii of gyration obtained were in excellent agreement with values reported in the literature (Luzzati et al., 1961; Ueki et al., 1985).

Model Calculations. *In vacuo* radii of gyration were calculated from atomic coordinates both via the program X-Plor (Brünger, 1992) and with a Unix awk program. The program PQMS (Connolly, 1985) was used to compute molecular volumes from crystal structures, and the number of electrons associated with solvent-excluded volumes, N_v, was the PQMS volume in Å^3 times 0.334 electrons/Å^3. MAMA, which is part of the RAVE package (Kleywegt & Jones, 1993) was used as part of the process that led to the determination of centers of mass and radii of gyration of the solvent-excluded volumes of proteins. The solvent-excluded volume was generated as follows: a molecular envelope ("mask") was determined from atomic coordinates using MAMA by assigning all non-hydrogen atoms a radius of 1.62 Å; a 1-Å grid was laid on the space containing this volume, and its elements were scored as being either inside or outside the mask, scoring internal voids in the volume as inside. The volume, radius of gyration, and center of mass of this object were computed. Computations done with grids of varying coarseness verified that values for parameters describing the solvent-excluded volume are not changed significantly by employing grids finer than 1 Å. Mask-derived volumes were the same as molecular volumes determined by PQMS to within 0.6%.

Correcting for EF-G·GDP and Apo-EF-G Contaminants. The EF-G·GTP samples examined were contaminated with GDP at levels determined by HPLC analysis of the samples after SAXS data collection. The fraction of apo-EF-G present in the samples containing GMPPCP was calculated directly from the binding equations. The radius of gyration of a solution containing two equal-mass components, R_0, was taken to be related to the radii of gyration of its components, R_1 and R_2, as follows:

$$R_0^2 = \chi_1 R_1^2 + \chi_2 R_2^2$$

where χ_1 and χ_2 are the mole fractions of the respective components (Geiduschek & Holtzer, 1959). Since the radius of gyration of the minority species (say, R_2) was known from data obtained previously from pure solutions, the radius of gyration of the conformer of interest (R_1) could be calculated.

RESULTS

Nucleotide Binding. Quantitative knowledge of the affinity of effector ligands for their target protein is an essential part of any study that examines the dependence of protein conformation on ligand binding. Therefore, dissociation constants (K_d) were determined for the interaction of EF-G with each of the guanine nucleotides used (see Experimental Procedures). Under the conditions of our SAXS experiments, the dissociation constants of *T. thermophilus* EF-G for GDP, GTP, and GMPPCP were found to be 0.92, 14.1, and 790 μM, respectively. [Under somewhat different conditions, Kaziro and co-workers found the dissociation constants of GDP and GTP from *T. thermophilus* EF-G to be 0.67 and 12.5 μM, respectively (Arai et al., 1978).]

These dissociation constants reveal the existence of an important technical problem. Since GDP binds to EF-G much more tightly than the other nucleotides studied, its concentration must be strictly controlled in samples in which complexes with GTP or GMPPCP are to be examined. HPLC analysis of the commercial GMPPCP used revealed the presence of no GDP or GDP-like contaminants, and demonstrated its stability under the conditions of interest. Likewise, the GDP preparation used had no detectable amount of GTP.

Experiments with GTP proved more problematic. Commercial GTP preparations contain appreciable amounts of GDP, and the EF-G used was found to hydrolyze GTP in SAXS buffer at a rate of 2.6 mol of GTP per mole of EF-G per day. Although this rate is low, the amount of GDP produced was too large to be ignored. GDP was removed from SAXS samples by converting it back into GTP, using a regenerating system containing 2-phospho(enol)pyruvate and pyruvate kinase (see Experimental Procedures). The efficiency of this approach was verified by HPLC analysis of the nucleotides present in SAXS samples *after* data had been collected from them.

We calculate that the samples prepared with GDP had >99% of the EF-G present bound to GDP. In the samples containing GMPPCP, 80% of the EF-G was complexed to that nucleotide, the remainder being apo-EF-G. Depending on the concentration of EF-G, the level of GDP in the samples containing the GTP regeneration system (measured after measurements were complete) varied from 2 to 5% that of GTP, which implies that not less than 71−88% of the EF-G present had GTP bound, the rest being EF-G·GDP.

Radius of Gyration. Since the concentration of protein present was small in these samples, no effort was made to correct for excluded volume effects; the protein scattering curves analyzed are the differences between protein solution and buffer scatter. Figure 1 shows $\ln(I(q))$ versus q^2 plots of the low-angle portions of representative scattering profiles for several concentrations of EF-G under the four conditions described above. The straight lines drawn through each data set are the variance-weighted, least-squares fits to their low-angle regions. Their slopes are proportional to the square of the radius of gyration of the protein (Guinier & Fournet,

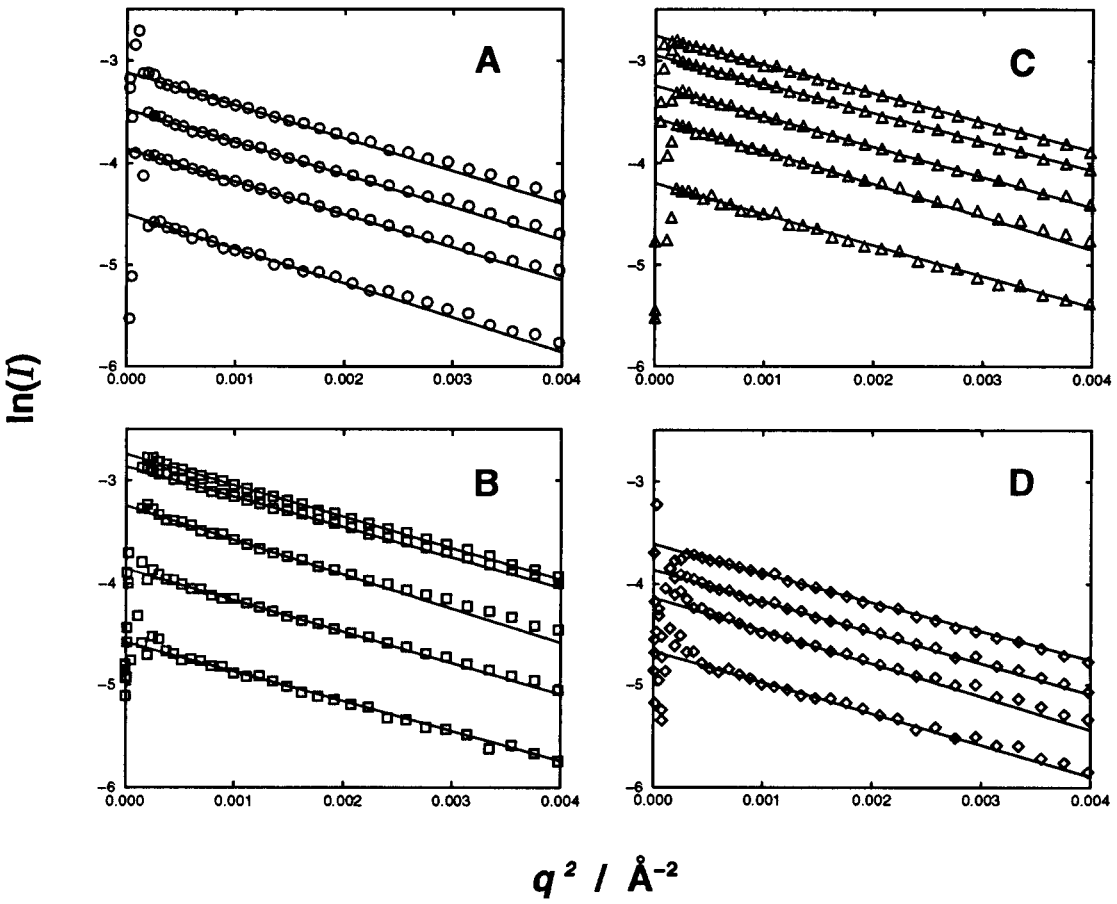

FIGURE 1: Guinier plots of representative scattering data from solutions of apo-EF-G (panel A, circles), EF-G·GDP (panel B, squares), EF-G·GMPPCP (panel C, triangles), and EF-G·GTP (panel D, diamonds).

Table 1: Radii of Gyration of the EF-G Samples[a]

nucleotide present	radius of gyration (standard deviation) (in Å)	
	Guinier plot	Fourier inversion
none	31.4 (0.7)	32.5 (0.5)
GDP	31.4 (0.7)	31.3 (0.5)
GTP (uncorrected)	32.6 (1.2)	30.4 (0.6)
GTP (corrected for EF-G·GDP)	32.9 (1.5)	30.2 (0.8)
GMPPCP (uncorrected)	31.6 (0.6)	32.2 (0.4)
GMPPCP (corrected for apo-EF-G)	31.7 (0.8)	32.2 (0.6)

[a] The radii of gyration reported were determined by extrapolating values measured at finite concentrations to zero concentration by using a variance-weighted linear regression algorithm. Samples were corrected for a minority conformation as described in the text.

1955). It is obvious that the radius of gyration of EF-G does not depend strongly on concentration and that the differences in the radii of gyration between the several forms of EF-G examined are small. Radii of gyration were also determined by computing the second moments of the length distributions obtained by Fourier inversion of each data set. They were the same as those found by Guinier's method, within experimental uncertainty. (Extrapolated forward scatters were consistent with the known molecular mass of EF-G.)

The radii of gyration obtained for EF-G at different concentrations in each of the four conditions were extrapolated linearly to zero concentration with the result shown in Table 1. They are nearly equal. The experimental radii of gyration of the samples containing GTP and GMPPCP, corrected for their content of EF-G·GDP and apo-EF-G, respectively, as described in Experimental Procedures, are also listed in Table 1 and (not unexpectedly) differ very little from their uncorrected values.

Models for EF-G in Solution. What would the radius of gyration of EF-G be if its conformation in solution were the same as it is when it is crystallized with no nucleotide or complexed with GDP? This question can be answered, at least approximately, because crystal structures exist for both forms of the molecule (Ævarsson et al., 1994; Czworkowski et al., 1994). Unfortunately, electron density for both crystals is so poor in the region of the third domain that the structure of that region can be only crudely modeled. In order to improve the model for domain 3, a replica of domain 5 was placed in the electron density of that part of the map. Domain 5 was chosen because it is an α/β domain, as domain 3 seems to be, and has nearly the same mass as the crudely modeled region. All the computations described below were done using this augmented model for EF-G. (Computational tests demonstrated that the inclusion of an ersatz domain 3 had little impact on the parameters calculated.)

When EF-Tu changes from its GTP form to its GDP form, its second and third domains translate and rotate as a rigid body relative to its G domain. Our putative EF-Tu·GDP-like EF-G conformation was produced by requiring that the second domain of EF-G move the same way its homologue does in EF-Tu, relative to its G domain, and that EF-G's third, fourth, and fifth domains move with the second domain as a rigid body. As Figure 2 shows, a huge conformational change results. As with EF-Tu, much of the molecule's mass moves away from its prior center of mass. The *in vacuo* radius of gyration of the nucleotide-free and GDP forms of

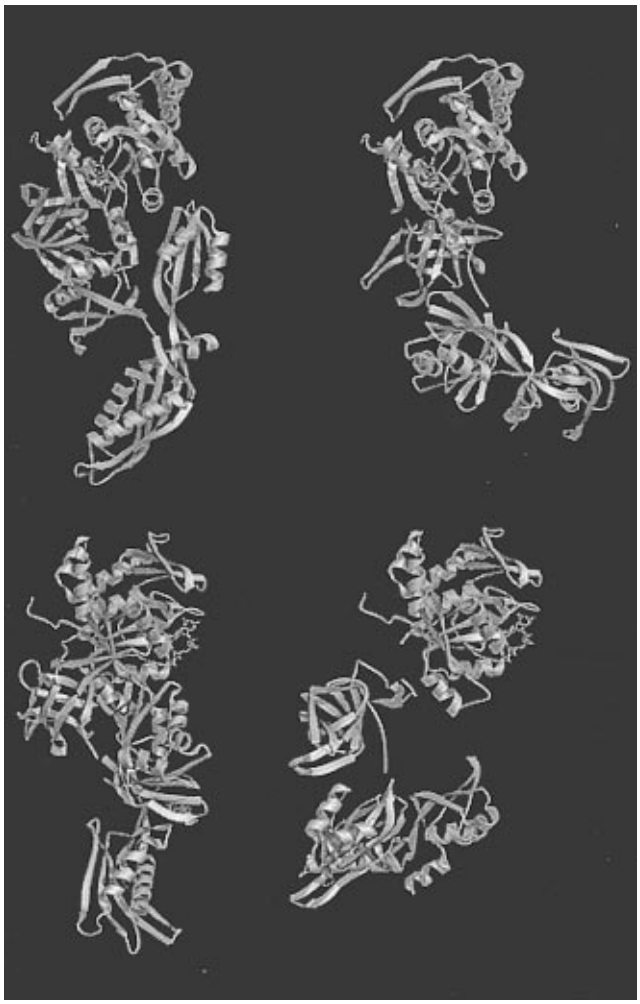

FIGURE 2: Comparison of the structures of EF-G·GDP (left) and a hypothetical model for EF-G·GTP (right). Left-right pairs of molecules are aligned on their G domains. Top−bottom pairs differ by a rotation of 90° about the vertical axis. (Note that the bound nucleotide is toward the viewer in the top depictions and at the right in the bottom depictions.) Images of EF-G models were made with the programs MOLSCRIPT (Kraulis, 1991) and Raster3D (Bacon & Anderson, 1988; Merritt & Murphy, 1994).

Table 2: Computed Radii of Gyration for EF-G Crystal Structures and the Hypothetical Model[a]

molecule	R_{vac} (Å)	R_{vol} (Å)	N_t	N_v	Δ (Å)	R_{sol} (Å)
apo-EF-G	31.39	31.01	39 559	28 715	0.493	32.35
EF-G·GDP	31.63	31.32	39 942	29 043	0.483	32.45
"EF-G·GTP"	36.11	35.93	39 213	28 513	0.459	36.58

[a] R_{vac} is the radius of gyration expected for EF-G *in vacuo*, computed from atomic coordinates as described in Experimental Procedures. R_{vol} is the radius of gyration of the solvent-excluded region. N_t is the total number of electrons in EF-G, and N_v is the number of electrons the volume occupied by the protein would contain if it were filled with water. Δ is the separation between the center of electron density of the protein and the center of mass of the solvent region it displaces. R_{sol} is the estimate for the solution radius of gyration of the protein deduced from these values, as described in the text. Estimates for apo-EF-G and EF-G·GDP are based on crystal structure coordinates. "EF-G·GTP" refers to the hypothetical model described in the text.

EF-G should both be about 31 Å, while that of the putative EF-G·GTP form of the molecule should be around 36 Å (Table 2).

Correction for the Contribution of Solvent to the Radius of Gyration. It is straightforward to calculate the *in vacuo* radius of gyration of a molecule from its atomic coordinates. By weighting distances between atoms by the product of their atomic numbers, an estimate appropriate for X-ray scattering can be obtained. (Differences between atomic number-weighted and atomic mass-weighted *in vacuo* radii of gyration for proteins are small.) However, even if the conformation of a protein does not change when its crystal dissolves, the radius of gyration calculated this way need not correspond exactly to what is measured in solution due to excluded volume effects and perturbed solvent structures immediately surrounding the protein [see Svergun et al. (1995)].

The size of the solvent-excluded volume of EF-G, the position of its center of mass and its radius of gyration were determined from the protein's crystal structure as described in Experimental Procedures. This information was combined with the protein's *in vacuo* radius of gyration to compute an estimate for its radius of gyration in solution by using the parallel axis theorem (Engelman & Moore, 1975)

$$R^2_{vac} = (N_v/N_t)R^2_{vol} + ((N_t - N_v)/N_t)R^2_{sol} + ((N_t - N_v)(N_v/N^2_t)\Delta^2$$

where R_{vac} is the radius of gyration computed from crystal structure coordinates, R_{vol} is the radius of gyration of the excluded volume, and R_{sol} is the radius of gyration predicted for the protein in solution. N_v is the total number of electrons the excluded volume would contain if it were full of solvent (N_v = volume × 0.334 electrons/Å^3). N_t is the total number of electrons in the protein itself, and Δ is the distance between the center of mass of the protein and the center of mass of the excluded volume. Rearrangement of the preceding equation yields

$$R^2_{sol} = (N_t/(N_t - N_v))R^2_{vac} - (N_v/(N_t - N_v))R^2_{vol} - (N_v/N_t)\Delta^2$$

The radius of gyration predicted for EF-G·GDP is almost the same as that of nucleotide-free EF-G, but is more than 4 Å smaller than that predicted for EF-G·GTP, were the latter to undergo a conformational rearrangement comparable to that seen in the crystal structures of EF-Tu·GDP and EF-Tu·GTP (Table 2). Note that the partial specific volume for EF-G estimated from its amino acid composition (Zamyatnin, 1972), 0.739 cm^3/g, implies an excluded volume of 91 629 Å^3. This is only 5% larger than our estimate (86 954 Å^3), supporting the plausibility of our excluded volume computations.

Length Distributions. As Figure 3 documents, the length distributions of the four states of EF-G studied are very similar, and each of the experimental length distributions resembles the computed length distribution for crystalline EF-G·GDP, not the length distribution computed for the hypothetical EF-G·GTP model. It is apparent from Figure 3 that the difference in radius of gyration between the two EF-G models reflects a striking difference in length distributions. By comparison with the GDP form of EF-G, the hypothetical EF-G·GTP model is strongly enriched for longer distances but has a maximum vector length that is only slightly (about 4 Å) greater. The number of vectors with length longer than 110 Å is very small for both forms of EF-G, and it is interesting that, while there are interatomic

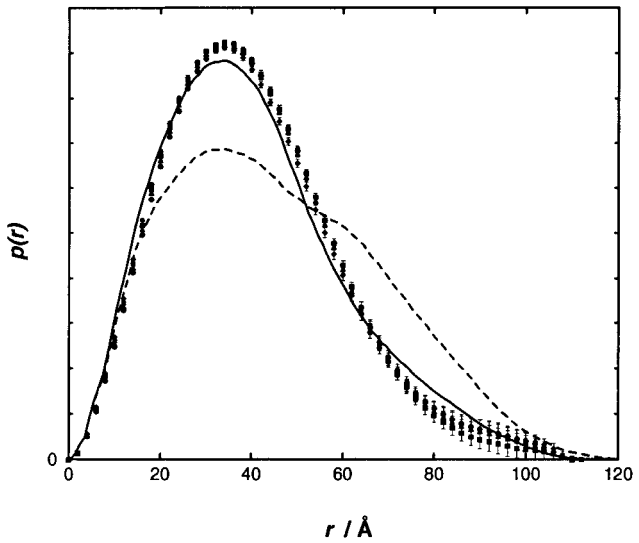

FIGURE 3: Length distributions derived from the scattering data of the lowest concentration samples are depicted with symbols: apo-EF-G, ●; EF-G·GDP, ■; EF-G·GMPPCP, ▲; EF-G·GTP, ◆. (The length distributions derived from the scattering profiles of more concentrated samples were nearly identical.) The length distribution calculated for the EF-G·GDP crystal structure is shown as a solid line, and that calculated for the hypothetical EF-G·GTP model is shown as a dashed line.

distances in the crystal structure of EF-G·GDP between 115 and 120 Å, they are so rare that they have almost no impact on the overall length distribution.

Thus the length distribution data and the radius of gyration data agree: the gross conformations of the four forms of EF-G are nearly identical in solution and virtually indistinguishable from crystalline EF-G·GDP.

DISCUSSION

Even though it is difficult to account properly for solvent contributions to the X-ray scattering of macromolecules, experience shows that, provided crystallization is not associated with a conformational change, experimental radii of gyration will agree with radii of gyration computed from crystal coordinates to within about 1 Å for proteins of moderate size (Svergun et al., 1995; Moore, 1982), which is what we find here. In addition, ligand-induced protein conformational changes can be detected by SAXS methods. In some instances solution data have confirmed the existence of changes identified initially by crystallography, e.g., the oxy−deoxy difference in hemoglobin (Conrad et al., 1969; Schneider et al., 1969) and the glucose-induced change in hexokinase (McDonald et al., 1979). In the latter case, the radius of gyration of hexokinase determined by SAXS decreased from 24.7 to 23.8 Å upon binding glucose, a decrease equal in magnitude to the difference between the *in vacuo* radii of gyration of the corresponding crystal structures (from 23.7 to 22.8 Å) but tiny compared to the change possible here. In other cases, higher resolution methods have subsequently explained conformational changes first detected by solution scattering (Heidorn & Trewhella, 1988).

Several studies have addressed the structure of EF-Tu via solution scattering (Österberg et al., 1981, 1986; Antonsson et al., 1986; Serdyuk et al., 1994). Analyses of its GDP form are in reasonable agreement with its crystal structure, but the results of studies of its GTP form have been rather variable. In none of these papers is a direct comparison of the two forms made. It is hard to comment on the discrepancies.

The data reported above show that the gross conformation of EF-G in solution is independent of the identity of the nucleotide bound to it, and closely similar to that expected if its solution conformation were identical to that found in crystals of apo-EF-G and EF-G·GDP. Since an EF-Tu-like conformational change would cause an increase in EF-G's radius of gyration by about 5 Å and a significant alteration in the appearance of its length distribution profile, we conclude that no such conformational change occurs in EF-G. It should be emphasized that the data *do not* rule out small-scale, nucleotide-dependent variations in EF-G structure. We would expect that the species of nucleotide bound to EF-G has some effect on the protein's structure, which in turn modifies its ribosome-binding affinity and its propensity to effect translocation.

It is interesting to note that there are indications that the conformation of EF-G bound to the ribosome may not be the same as it is in solution. For example, twenty years ago Bodley and co-workers found that the effective dissociation constant K_d of GMPPCP complexed with *E. coli* EF-G and ribosomes is 59 nM (Baca et al., 1976), which is almost 25 times less than the K_d for the interaction of GTP with EF-G from *T. thermophilus* in the absence of ribosomes, and over 1000 times less than the K_d for the interaction of GMPPCP with *T. thermophilus* EF-G in the absence of ribosomes. Either the conformation of the nucleotide binding site of EF-G changes when EF-G binds to the ribosome, or ribosomal components contribute to nucleotide binding, or both. That ribosome-bound EF-G might differ significantly in conformation from free EF-G is also indicated by the observation that fusidic acid binds only to EF−G−ribosome complexes (Willie et al., 1975), but that all known fusidic acid-resistant mutants are mutants in EF-G (Johanson et al., 1996).

A great deal of new information about translocation has emerged in the last decade, and it is not hard to assemble it into a consistent explanation for how EF-G might work (Figure 4). We start by assuming that EF-G·GTP is indeed a mimic of the EF-Tu ternary complex, as the data presented above imply, and follow the hybrid-sites model for the elongation cycle proposed by Noller and his colleagues (Moazed & Noller, 1989). In their model, peptide transfer is accompanied by movement of the amino acid accepting end of A-site bound tRNAs from the large subunit A site, where EF-Tu puts them, to the large subunit P site, and by simultaneous movement of the amino acid accepting end of the tRNA in the P site from the large subunit P site to the large subunit E site. Since the anticodon ends of both tRNAs remain stationary with respect to the small subunit, hybrid states are created, the most important being that of the newly created peptidyl tRNA. Its anticodon end occupies the small subunit A site, and its aminoacyl end fills the large subunit P site. Thus the hybrid sites model suggests that only the positions of the anticodon stems of tRNAs on the small subunit change during the EF-G-promoted translocation reaction.

After EF-Tu delivers an aminoacyl tRNA to the ribosome and the nascent peptide has been transferred, the ribosome is in the pre-translocational state. The tRNA movement postulated to accompany peptide transfer opens up the region

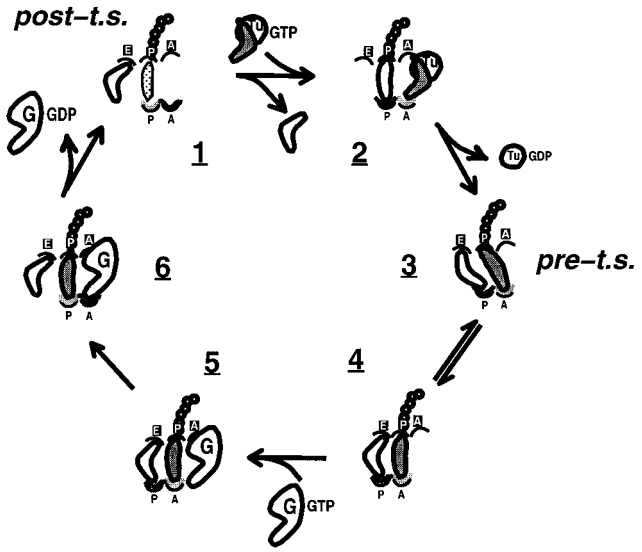

FIGURE 4: A model for EF-G-promoted translocation within the peptide elongation cycle. Large subunit half-sites are shown at the top of the tRNAs, labeled with white letters E, P, and A; small-subunit half-sites are below the tRNAs and are labeled with black letters P and A. Beginning with the ribosome in the post-translocational state (1), the ternary complex binds, deposits cognate aminoacyl tRNA in the A site (2), hydrolyzes GTP and departs, leaving the ribosome in the pre-translocational state (3), where tRNAs are bound in hybrid states. An equilibrium exists between 3 and a more open conformation of the ribosome (4); the latter conformation permits the binding of EF-G to the ribosome, as discussed in the text (5). A motion of all or part of the small subunit relative to the large reconstitutes the complete, "ternary complex-ready" A site, while EF-G remains fixed to the large subunit (6). After this state is achieved and EF-G's bound GTP has been hydrolyzed to GDP, EF-G's affinity for the ribosome is greatly reduced and it dissociates from the ribosome.

of the large subunit where the EF-G domains that mimic the aminoacyl stem of tRNA must bind, but since the anticodon end of a tRNA remains in the small-subunit A site, the fourth domain of EF-G, which resembles the anticodon stem of tRNA, cannot be accommodated. The only way EF-G can bind is if all or part of the small subunit moves relative to the large subunit, carrying with it the anticodon stem of the tRNA bound to its A site. A clam-shell-like opening of the gap between the two ribosomal subunits that moved the anticodon stem by about 20 Å would suffice, but there are many other possibilities. (It is likely that the motions required happen in the absence of factors because translocation can occur in the absence of EF-G, albeit at a very slow rate.) If EF-G were to bind to the ribosome when the ribosome is "open" this way, it would be impossible for the small subunit to return to its original position until the anticodon end of the tRNA in the small-subunit A site moved to the small-subunit P site, and hence that motion would be promoted by EF-G binding. Interactions between the small-subunit A site and EF-G's fourth domain might also favor the return of the ribosome to the "closed" state. Assuming that mRNAs are pulled passively across the surface of the ribosome because of their interactions with tRNAs, as has been suggested in the past (Belitsina et al., 1981), translocation is explained.

For many years it was believed that the GTP hydrolysis catalyzed by EF-G occurs after translocation. This idea was consistent with the observation that EF-G promotes one round of translocation in the presence of nonhydrolyzable analogues of GTP, and with the hypothesis that the purpose of GTP hydrolysis is to facilitate the release of EF-G from the ribosome after translocation. Kinetic data recently published by Wintermeyer and his colleagues indicates that GTP hydrolysis may *precede* elongation, and this has led to the suggestion that EF-G is a "molecular motor" that couples the energy of GTP hydrolysis directly translocation (Rodnina et al., 1997; Cross, 1997). We are unsure what a "molecular motor" is, but we are sure that these new observations do not require that translocation be coupled directly to GTP hydrolysis. If translocation is coupled to GTP hydrolysis, why does EF-G·GMPPCP promote translocation at all?

The concept that the factor release is the function of GTP hydrolysis is easily rescued by postulating that EF-G cannot be released from the ribosome unless it has a GDP in its nucleotide binding site, and its fourth domain has interacted with the A site of the 30S subunit. Since the second condition for release will not be met until after translocation, EF-G release will follow translocation. (In fact, for mechanisms of this type, the timing of GTP hydrolysis relative to translocation is unimportant.)

In support of the proposal being advanced here, we note that the role of GTP hydrolysis in all other G proteins is believed to be modulation of binding affinities. Thus if EF-G were to couple GTP hydrolysis directly to a mechanical process, the implication would be that despite all its similarities to other G proteins, it is not a G protein. Also noteworthy in this regard are recent studies showing that unidirectional macromolecular motion and force can result when macromolecules bind, with an affinity modulated by nucleotide hydrolysis, to surfaces with a nonuniform interaction potential (Astumian & Bier, 1996; Guajardo & Sousa, 1997). Direct coupling is unnecessary.

The final issue that needs to be confronted is factor competition and interference. If EF-G really is a mimic of the ternary complex, one would anticipate that noncognate ternary complexes might promote translocation just the way EF-G does, a notion pregnant with evolutionary implications. While there are hints that this may occur with cognate ternary complexes (Bergemann & Nierhaus, 1983), it has not been demonstrated with noncognate complexes. (Poor mRNA/anticodon interactions may reduce the importance of this kind of competition between noncognate ternary complexes and EF-G *in vivo*.) The potential for competition between EF-G·GTP and the EF-Tu ternary complex for post-translocational ribosomes seems more serious. If it were to occur, it would slow the rate at which ribosomes select aminoacyl tRNAs, and could easily lead to the unproductive hydrolysis of GTP. The only mechanisms we can imagine for controlling this problem all involve modest, translocation-dependent changes in the factor binding site on the ribosome that modulate its affinity for the two factors. In pre-translocational ribosomes, the affinity of the site for ternary complex would be low and its affinity for EF-G high. In post-translocational ribosomes relative affinities are reversed. Cycle-dependent alterations in ribosome conformation that affect factor binding this way are consistent with the recent observation of Mesters et al. (1994) that the ribosome-dependent GTPase activities of EF-Tu and EF-G are enhanced by the presence of the other factor, in the absence of tRNA.

Several additional observations are accommodated by this model. For example, it is easy to understand why translocation is promoted (inefficiently) by EF-G·GDP (Rodnina

et al., 1997). It has the same overall shape as EF-G·GTP and should bind (weakly) to the same site on the ribosome. In addition, as one might expect, truncated versions of EF-G that lack domain 4 possess a ribosome-stimulated GTPase similar to that of intact EF-G but are even less efficient at promoting translocation than EF-G·GDP. Moreover, truncated EF-G is not released from the ribosome by GTP hydrolysis, consistent with the proposal that release depends on interactions involving domain 4 (Rodnina et al., 1997). Finally, unlike many other models for the elongation cycle, this model predicts that, except for the placement of tRNAs, at moderate resolution, pre-translocational ribosomes should look just like post-translocational ribosomes, and this is exactly what has been reported recently (Stark et al., 1997).

The model for translocation outlined above is by no means the only one that can be proposed at this point. However, it is as simple a model as can be advanced that is consistent with the following postulates: (1) that the half-sites scheme for elongation is correct, (2) that EF-G·GTP is a ternary complex mimic, the critical point supported by the data presented above, (3) that translocation does not depend on changes in the gross conformation of EF-G, and (4) that the guanine nucleotides bound to EF-G serve only as modulators of the factor's affinity for the ribosome.

ACKNOWLEDGMENT

We acknowledge the support and encouragement of Dr. Thomas A. Steitz, and thank Dr. Zimei Bu for her help with the use of the small-angle X-ray scattering instrument. We are grateful to Mrs. Betty Freeborn for her assistance with protein purifications. Dr. Morten Kjeldgaard supplied the coordinates of EF-Tu, and apo-EF-G coordinates were supplied by Dr. Anders Liljas.

REFERENCES

Ævarsson, A., Brazhnikov, E., Garber, M., Zheltonosova, J., Chirgadze, Y., al-Karadaghi, S., Svensson, L. A., & Liljas, A. (1994) *EMBO J. 13*, 3669−3677.

Antonsson, B., Leberman, R., Jacrot, B., & Zaccai, G. (1986) *Biochemistry 25*, 3655−3659.

Arai, K., Kawakita, M., & Kaziro, Y. (1974) *J. Biochem. 76*, 283−292.

Arai, K., Arai, N., Nakamura, S., Oshima, T., & Kaziro, Y. (1978) *Eur. J. Biochem. 92*, 521−531.

Astumian, R. D., & Bier, M. (1996) *Biophys. J. 70*, 637−653.

Baca, O. G., Rohrbach, M. S., & Bodley, J. W. (1976) *Biochemistry 15*, 4570−4574.

Bacon, D. J., & Anderson, W. F. (1988) *J. Mol. Graphics 6*, 219−220.

Belitsina, N. V., Tnalina, G. Z., & Spirin, A. S. (1981) *FEBS Lett. 131*, 289−292.

Berchtold, H., Reshetnikova, L., Reiser, C. O. A., Schirmer, N. K., Sprinzl, M., & Hilgenfeld, R. (1993) *Nature 365*, 126−132.

Bergemann, K., & Nierhaus, K. H. (1983) *J. Biol. Chem. 258*, 15105−15113.

Blank, J., Grillenbeck, N. W., Kreutzer, R., & Sprinzl, M. (1995) *Protein Exp. Purif. 6*, 637−645.

Bodley, J. W., & Lin, L. (1970) *Nature 227*, 60−62.

Bourne, H. R., Sanders, D. A., & McCormick, F. (1991) *Nature 349*, 117−127.

Brünger, A. (1992) *X-Plor, Version 3.1. System for X-Ray Crystallography and NMR*, Yale University Press, New Haven, CT.

Connolly, M. L. (1985) *J. Am. Chem. Soc. 107*, 1118−1124.

Conrad, H., Mayer, A., Thomas, H. P., & Vogel, H. (1969) *J. Mol. Biol. 41*, 225−229.

Cross, R. A. (1997) *Nature 385*, 18−19.

Czworkowski, J., Wang, J., Steitz, T. A., & Moore, P. B. (1994) *EMBO J. 13*, 3661−668.

Engelman, D. M., & Moore, P. B. (1975) *Annu. Rev. Biophys. Bioeng. 4*, 219−241.

Geiduschek, E. P., & Holtzer, A. (1959) *Adv. Biol. Med. Phys. 6*, 431−551.

Gill, S. C., & von Hippel, P. H. (1989) *Anal. Biochem. 182*, 319−326.

Guajardo, R., & Sousa, R. (1997) *J. Mol. Biol. 265*, 8−19.

Guinier, A., & Fournet, G. (1955) *Small-Angle Scattering of X-Rays*, John Wiley and Sons, New York.

Heidorn, D. B., & Trewhella, J. (1988) *Biochemistry 27*, 909−915.

Johanson, U., Ævarsson, A., Liljas, A., & Hughes, D. (1996) *J. Mol. Biol. 258*, 420−432.

Kjeldgaard, M., & Nyborg, J. (1992) *J. Mol. Biol. 223*, 721−742.

Kjeldgaard, M., Nissen, P., Thirup, S., & Nyborg, J. (1993) *Structure 1*, 35−50.

Kleywegt, G. J., & Jones, T. A. (1993) *ESF/CCP4 Newsl. 28*, 56−59.

Kraulis, P. J. (1991) *J. Appl. Crystallogr. 24*, 946−950.

Liljas, A. (1996) *Curr. Biol. 6*, 247−249.

Luzzati, V., Witz, J., & Nicolaieff, A. (1961) *J. Mol. Biol. 3*, 379−392.

Maniatis, T., Fritsch, E. F., & Sambrook, J. (1982) *Molecular Cloning*, 1st ed., Cold Spring Harbor Laboratory Press, Plainview, NY.

McDonald, R. C., Steitz, T. A., & Engelman, D. M. (1979) *Biochemistry 18*, 338−342.

Merritt, E. A., & Murphy, M. E. P. (1994) *Acta Crystallogr. D50*, 869−873.

Mesters, J. R., Potapov, A. P., Degraaf, J. M., & Kraal, B. (1994) *J. Mol. Biol. 242*, 644−654.

Miller, D. L. (1972) *Proc. Natl. Acad. Sci. U.S.A. 69*, 752−755.

Moazed, D., & Noller, H. F. (1989) *Nature 342*, 142−148.

Moore, P. B. (1980) *J. Appl. Crystallogr. 13*, 168−175.

Moore, P. B. (1982) in *Methods of Experimental Physics* (Ehrenstein, G., & Lecar, H., Eds.) pp 337−390, Academic Press, New York.

Nissen, P., Kjeldgaard, M., Thirup, S., Polekhina, G., Reshetnikova, L., Clark, B. F., & Nyborg, J. (1995) *Science 270*, 1464−1472.

Österberg, R., Sjöberg, B., Ligaarden, R., & Elias, P. (1981) *Eur. J. Biochem. 117*, 155−159.

Österberg, R., Elias, P., Kjems, J., & Bauer, R. (1986) *J. Biomol. Struct. Dyn. 3*, 1111−1120.

Porod, G. (1951) *Kolloid. Z. 124*, 83−114.

Richman, N., & Bodley, J. W. (1972) *Proc. Natl. Acad. Sci. U.S.A. 69*, 686−689.

Richter, D. (1972) *Biochem. Biophys. Res. Commun. 46*, 1850−1856.

Rodnina, M. V., Savelsbergh, A., Katunin, V. I., & Wintermeyer, W. (1997) *Nature 385*, 37−41.

Rose, R. K., & Hogg, S. D. (1995) *Biochim. Biophys. Acta 1245*, 94−98.

Schneider, R., Mayer, A., Schmatz, W., Kaiser, B., & Scherm, R. (1969) *J. Mol. Biol. 41*, 231−235.

Serdyuk, I. N., Pavlov, M. Y., Rublevskaya, I. N., Zaccai, G., & Leberman, R. (1994) *Biophys. Chem. 53*, 123−130.

Smith, C. K., Bu, Z., Anderson, K. S., Sturtevant, J. M., Engelman, D. M., & Regan, L. (1996) *Protein Sci. 5*, 2009−2019.

Stark, H., Orlova, E. V., Rinke-Appel, J., Jünke, N., Mueller, F., Rodnina, M., Wintermeyer, W., Brimacombe, R., & van Heel, M. (1997) *Cell 88*, 19−28.

Svergun, D., Barberato, C., & Koch, M. H. J. (1995) *J. Appl. Crystallogr. 28*, 768−773.

Ueki, T., Hiragi, Y., Kataoka, M., Inoko, Y., Amemiya, Y., Izumi, Y., Tagawa, H., & Muroga, Y. (1985) *Biophys. Chem. 23*, 115−124.

Willie, G. R., Richman, N., Godtfredsen, W. O., & Bodley, J. W. (1975) *Biochemistry 14*, 1713−1718.

Winzor, D. J., & Sawyer, W. H. (1995) *Quantitative Characterization of Ligand Binding*, Wiley-Liss, Inc., New York.

Zamyatnin, A. A. (1972) *Progr. Biophys. Mol. Biol. 24*, 107−123.

BI970610K